A Comparative Study of Correlation Methods in Functional Connectivity Analysis Using fMRI Data of Alzheimer's Patients

Hessam Ahmadi[1], Emad Fatemizadeh[2]*, Ali Motie-Nasrabadi[3]

[1]PhD Candidate, Department of Biomedical Engineering, Science and Research Branch, Islamic Azad University, Tehran, Iran
[2]PhD, School of Electrical Engineering, Sharif University of Technology, Tehran, Iran
[3]PhD, Department of Biomedical Engineering, Shahed University, Tehran, Iran

ABSTRACT

Background: Functional Magnetic Resonance Imaging (fMRI) is a non-invasive neuroimaging tool, used in brain function research and is also a low-frequency signal, showing brain activation by means of Oxygen consumption.

Objective: One of the reliable methods in brain functional connectivity analysis is the correlation method. In correlation analysis, the relationship between two time-series has been investigated. In fMRI analysis, the Pearson correlation is used while there are other methods. This study aims to investigate the different correlation methods in functional connectivity analysis.

Material and Methods: In this analytical research, based on fMRI signals of Alzheimer's Disease (AD) and healthy individulas from the ADNI database, brain functional networks were generated using correlation techniques, including Pearson, Kendall, and Spearman. Then, the global and nodal measures were calculated in the whole brain and in the most important resting-state network called Default Mode Network (DMN). The statistical analysis was performed using non-parametric permutation test.

Results: Results show that although in nodal analysis, the performance of correlation methods was almost similar, in global features, the Spearman and Kendall were better in distinguishing AD subjects. Note that, nodal analysis reveals that the functional connectivity of the posterior areas in the brain was more damaged because of AD in comparison to frontal areas. Moreover, the functional connectivity of the dominant hemisphere was disrupted more.

Conclusion: Although the Pearson method has limitations in capturing non-linear relationships, it is the most prevalent method. To have a comprehensive analysis, investigating non-linear methods such as distance correlation is recommended.

Keywords

Functional Connectivity; Correlation; Brain Networks; Fmri; Graph Measures; DMN Network; Alzheimer Disease; Brain; Neuroimaging

Introduction

Functional Magnetic Resonance Imaging (fMRI) has been recently become more popular in brain function studies. During the fMRI examination, the low-frequency fluctuations called Blood Oxygen Level Dependent (BOLD) signal that shows the oxygen consumption of the brain regions, has been recorded [1]. In brain research, there

*Corresponding author:
Emad Fatemizadeh
School of Electrical Engineering, Sharif University of Technology, Tehran, Iran
E-mail: fatemizadeh@sharif.edu

Received: 4 July 2020
Accepted: 7 September 2020

are three types of brain connectivity called structural, functional, and effective. The temporal correlation of fMRI signals shows the functional connectivity in the brain that could be among all voxels (that is very time-consuming) or Regions of Interest (ROI) [2]. Several functional connectivity studies based on fMRI signals show that different pathological or physiological conditions affect the brain functional connectivity [3-5]. There are several methods to calculate the correlation between time-series, including Pearson Correlation Coefficient (PCC), Kendall, and Spearman. All the methods are popular in literature but the PCC is the most common method used in fMRI functional connectivity analysis [6].

Alzheimer's Disease (AD) that is the most common type of dementia, is a neurodegenerative illness, disrupting the performance of the brain and the normal life of the patient in the final stages of the disease. Official deaths authentications recorded 122,019 deaths from AD in 2018, making Alzheimer's the 6th and 5th main reason for death in the United States and among Americans age 65 and older, respectively [7]. Accordingly, using fMRI signals to study AD is very popular and also helpful for all the people involved in this issue directly or indirectly [8].

Studies on AD shows that the functional connectivity of the brain and especially main brain networks such as Default Mode Network (DMN) has decreased [9, 10]. Classification AD patients from the healthy individulas is another popular topic that has been performed using different features and dimension reduction algorithms, and a wide range of classifiers, including K-Nearest Neighbors, Artificial Neural Networks (ANN) and Support Vector Machine (SVM) [11-13]. There are also several studies on the early stage of the disease called Mild Cognitive Impairment (MCI) [14, 15]. Besides, using additional information such as MRI, structural images has been investigated [16]. In functional connectivity analysis, non-linear methods such as mutual information have been used as well [17]. The study of the functional connectivity using coherence analysis [18] or comparing the effect of AD and normal aging in the functional connectivity was done before [19]. Moreover, some studies especially focused on white matter functional connectivity [20] or some brain networks or ROIs [21].

As mentioned above the functional connectivity analysis is very common and popular among researchers. Although there are many ways to compute the functional connectivity, the most common method for analyzing functional connectivity is Pearson Correaltion Coefficient (PCC). PCC is conducted uisng the linear correlation; however, in non-linear relationships, this method is weak. Besides, there anot enough studies that compare the result of the different correlation methods to PCC. In this study, functional connectivity matrices are generated using different correlation methods, including PCC, Spearman, and Kendall, to explore the performance of these methods in brain functional connectivity analysis in AD subjects.

In the materials and methods section, the database is introduced. Then the preprocessing step is explained and different correlation methods and their formulas are presented. After that, graph theory and feature extraction are proposed. In the result section, the statistical outcomes and different analysis findings are presented. Finally, the results are going to discuss in the last section. This study aims to investigate the different correlation methods in functional connectivity analysis.

Material and Methods

In this analytical research, the data and the tools used in this study are presented and explained completely. The flowchart of the study is shown in Figure 1.

Database

The fMRI data has been collected from the Alzheimer's Disease Neuroimaging Initiative

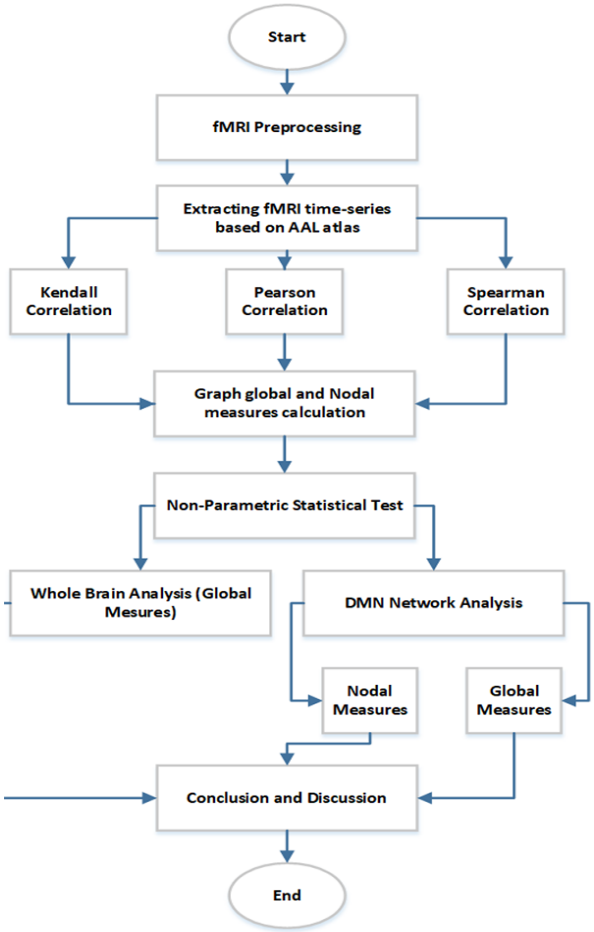

Figure 1: The flowchart of the study.

(ADNI) phase 2 [22, 23]. The data consists of 28 individulas for the AD group and 34 individulas for the control group. All the scans, including structural and functional images have been done by a 3 Tesla Philips MRI machine. The Repetition Time (TR) and Echo Time (TE) are 3000 msec and 30 msec, respectively. The flip angle was 80 and 3.3125 mm was the thickness of each slice [24]. The demographic information is depicted in Table 1.

Preprocessing

The preprocessing was done using the Data Processing Assistant for fMRI (DPARSF) toolbox in Matlab software [25]. The preprocessing consists of realignment that performed by a six parameter rigid body transformation. BY the last slice, the slice timings were corrected. Then the Montreal Neurological Institute (MNI) atlas has been used for data normalization. Data were passed through a bandpass filter (0.01-0.08 Hz) and smoothed by a Gaussian filter (FWHM=4 mm). Finally, to obtain the time-series, the Automated Anatomical Labeling (AAL) atlas, reliable in this field, has been employed. Based on AAL atlas, the brain parcellates into 116 distinct regions [26].

Correlations

After extracting fMRI signals based on AAL atlas, the correlations among time-series were computed to obtain brain functional connectivity. PCC is one of the main methods to calculate the correlation [27]. The formula of PCC is as follows:

$$\rho_{x.y} = \frac{\mathrm{cov}(x.y)}{\sigma_x \sigma_y} \qquad (1)$$

Where σ_x and σ_y correspond to the standard deviation of signal x and y, respectively. The PCC computes the linear correlation and the magnitude is between -1 to 1. The sign shows

Table 1: The information of the data. Mini-Mental State Examination (MMSE) and Clinical Dementia Rating (CDR) are two clinical exams performed for analysis the mental health in Alzheimer's Disease (AD).

Group	No. (Male/Female)	Age	Head Motion	MMSE Score	CDR Score
AD	(14/14)	74.9±4.9	0.32±0.09 mm	20.35±0.54	1.03±0.54
CN	(14/20)	74.1±4.3	0.22±0.14 mm	29.11±1.24	0.16±0.05

MMSE: Mini-Mental State Examination, CDR: Clinical Dementia Rating, AD: Alzheimer's Disease, CN: Control

the direction and the magnitude corresponds to the correlation power.

The Spearman correlation is another method, which is a nonparametric rank correlation between two variables, showing that how well the connection between two factors can be portrayed using a monotonic function [28]. For computation the Spearman correlation, the variables are firstly converted to rank variables and then the PCC formula (Equation 1) is performed.

Kendall coefficient is a non-parametric popular method for computing the correlation between two variables, quantifing the ordinal association between variables [29]. Assume that (x_i, y_i) and (x_j, y_j) are two coordintes with condition that if $x_i > x_j$ and $y_i > y_j$, they are concordant and if $x_i < x_j$ and $y_i < y_j$ they are discordant. Accordingly, the formula of the Kendall coefficient is as follows:

$$\tau = \frac{n_c - n_d}{\frac{n(n-1)}{2}} \qquad (2)$$

Where n_c and n_d correspond to the number of concordant and number of discordant pairs, respectively. Besides, n is the number of pairs.

Brain Networks and Graph Theory

In functional connectivity analysis, the brain is modeled as an undirected graph. In this graph, the brain ROIs correspond to the graph nodes and the functional connectivities between nodes were modeled as network edges. The edges of the graph demonstrates the functional connectivity (correlation) [30]. In mathematics, $G = (V, E)$ is a graph that E is the representatives of links and V corresponds to vertices. Besides, some studies sparsed the graphs by thresholding to remove weak links and noises. As this paper aims to compare the effect of different correlation methods, sparsification is not obliged. As this study focused on functional connectivity, the absolute value of negative correlations was considered for further analysis [31]. After generating weighted undirected graphs based on different correlation methods, graph global features were computed. The formula of graph measures is shown in Table 2.

In Table 2, n and $d_G(x.y)$ show the number of nodes and the distance between the x and y, respectively. The G^{Ideal} is the representative of a fully connected network. The l is the number of links and $A_{x.y}$ shows the connectivity matrix. $\delta_{x.y}$ is 0 if the x and y are from the same community. C_r and L_r correspond to an equivalent random graph. The average efficiency formula is $(G) = \frac{1}{n(n-1)} \sum_{x \neq y \in G} \frac{1}{p(x.y)}$, where $p(x.y)$ corresponds to the shortest path length between x and y.

Some measures are computed over a single node. These types of features demonstrate the performance of a single node in the network specifically. *Betweenness* measures the centrality in a network based on the shortest paths, and is the ratio of the shortest path (that crosses through a hub to the total number of shortest paths). Closeness is the inverse of the path length of a hub [33]. Participation estimates the connection between the number of edges associating a hub outside its locale and all of its outnumber of edges. The participation formula is:

$$P_i = 1 - \sum_s \left(\frac{K_{s_i}}{K_i} \right)^2 \qquad (3)$$

where s_i and K_i are the all outnumber of links of vertice i and K_{s_i} is the number of edges associating the vertice i inside Module (neighborhood).

Results

After generating weighted undirected functional brain networks and extracting graph features, statistical analysis was performed. Since there is no assumption about the distribution of the data, the non-parametric permutation test was implemented. The results of the statistical test are shown in Table 3 in terms of P-values. The bold numbers in Table 3 corre-

Table 2: The formula of graph global measures [32].

Graph Measure	Formula
Degree	-
Eccentricity	$Ecc = \max\{d_G(x.y)\}$
Strength	$Str(\upsilon) = \sum_{\upsilon \in V} E$
Radius	$R = \min\{ECC\}$
Diameter	$D = \max\{ECC\}$
Characteristics Path Length	$L = \frac{\sum_{x.y \in V(G)} d_G(x.y)}{n(n-1)}$
Global Efficiency	$E_{glob}(G) = \frac{E(G)}{E(G^{Ideal})}$
Local Efficiency	$E_{loc}(G) = \frac{1}{n}\sum_{x \in G} E(G_x)$
Clustering	$\frac{Number\ of\ closed\ triplets}{number\ of\ all\ triplets}$
Modularity	$M = \frac{1}{l}\sum_{x.y}\left[A_{x.y} - \frac{k_x k_y}{l}\right]\delta_{x.y}$
Transitivity	$T = \frac{3 \times number\ of\ triangles}{number\ of\ connected\ triples\ of\ nodes}$
Small-Worldness	$\sigma = \frac{C/C_r}{L/L_r}$

spond to the P-values < 0.05.

According to Table 3, the Pearson correlation shows significant changes in strength, characteristic path length, global efficiency, local efficiency, clustering, and transitivity features. In addition to the mentioned features, Spearman and Kendall correlations show significant changes in the modularity feature as well. Regardless of the features that show significant differences, generally, the P-values obtained from Kendall and Spearman were smaller in comparison to the Pearson method. It can be concluded that Kendall and Spearman are more powerful in the discrimination of Alzheimer's disease from the control group in terms of functional connectivity and graph

Table 3: P-values of the global features statistical test.

Features / Correlation	P-Values		
	Pearson	Spearman	Kendall
Degree	1	0.1586	0.1641
Strength	0.0026	0.0036	0.0023
Radius	0.2009	0.1689	0.2282
Diameter	0.4882	0.4483	0.4819
Eccentricity	0.3295	0.4118	0.4251
Charactristic Path Length	0.0112	0.0132	0.011
Global Efficiency	0.0018	0.0035	0.0031
Local Efficiency	0.0018	0.0223	0.0021
Clustering	0.006	0.0035	0.0028
Transitivity	0.0074	0.0031	0.0034
Modularity	0.057	0.0443	0.0395
Small Worldness	0.6274	0.2615	0.1484

measures.

The diameter and radius were computed based on the eccentricity feature, capturing the maximal distance between two nodes. Moreover, they did not show any significant changes. It can be interpreted that although Alzheimer's affects the brain function, the paths between ROIs that flowing information still exists. Accordingly, none of the brain ROIs is isolated from the rest of the brain. The small worldness architecture of the brain remains in this database. Since there was no sparsification step, it was expected that the degree feature indicates no significant differences.

The performance of different correlations methods has been analyzed through global graph measures. Since other studies [21, 34] reported functional connectivity changes in DMN to analyze more comprehensively, the measures in DMN were investigated. Furthermore, most of the global measures can be computed for a single node. On the other hand, some features, including small worldness related to the whole graph cannot be calculated for a node. First of all, the global measures that are available in the nodal analysis were extracted for every node of the DMN network. Consequently, there were ten charts for ten ROIs of the DMN. For example, Table 4 is for frontal superior medial left ROI. The boldface P-values in Table 4 shows a statistically significant difference.

In comparison among different correlation methods, based on the number of features displaying significant changes, Pearson, Spearman, and Kendall show a significant differ-

Table 4: P-values of the global features extracted for the node number 23 in the Automated Anatomical Labeling (AAL) atlas. The last column ranks the features in all Default Mode Network Regions of Interests (DMN ROIS) based on the number of significant changes.

Features / Correlation	P-Values			
	Pearson	Spearman	Kendall	Rank (In all ROI)
Strength	0.4324	0.3710	0.3881	4th
Eccentricity	0.1155	0.3318	0.2591	7th
Path Length	0.0012	0.0611	0.0014	3rd
Global Efficiency	0.1462	0.2702	0.2444	5th
Local Efficiency	0.0792	0.0924	0.0799	2nd
Clustering	0.0545	0.0605	0.0515	1st
Within Modularity	0.0626	0.1414	0.0625	6th

ROI: Regions of Interest

ence in 27, 32, and 33 features, respectively out of 70 features (7 different features in 10 ROIs). These results were similar to the global measures in the whole network (Table 3) and the Spearman and Kendall were more powerful in comparison to Pearson correlation.

The eccentricity feature like the whole-brain analysis has no significant difference in neither the ROIs nor correlation methods. On the other hand, clustering, local efficiency, and path length were the features, demonstrating the most significant differences respectively. Besides, the last column of Table 4 displays the ranks of the features based on their number of significant differences in all DMN ROIs.

Among the ROIs of the DMN network, the angular area (left and right) and cingulum posterior area (left and right) seemed to be more affected by the AD because more features showed significant difference and these results are in consistent with previous studies [35, 36]. Besides, the measures in the left hemisphere of the brain demonstrate more significant changes. Since all the subjects were right-handed, it can be concluded that the dominant hemisphere was affected more by the AD. Figure 2 exhibits the axial dorsal view of DMN ROIs, sorted based on their affection by AD.

As shown in Figure 2, it can be interpreted that the AD disrupts functional connectivity in posteriors ROI's of DMN network more in comparison to frontal ROI's.

Besides the global measures, there are some nodal measures computed only over a single node and do not define in the whole graph. These features were calculated in ROI's of DMN network separately and Table 5 illustrates the P-values for frontal superior medial left ROI. The boldface P-values in Table 5 exhibits a statistically significant difference.

All three correlation methods show significant difference in 18 features out of 40 (4 nodal measures on every 10 DMN ROIs); thus, regardless of the correlation method the performances of nodal measures extracted from graphs are the same.

Among four nodal measures, the triangles and closeness feature exhibits more significant changes and the betweenness demonstrates the least significant difference. It is worthwhile to mention that the ranks of ROIs based on nodal measures were as same as global measures (Figure 2).

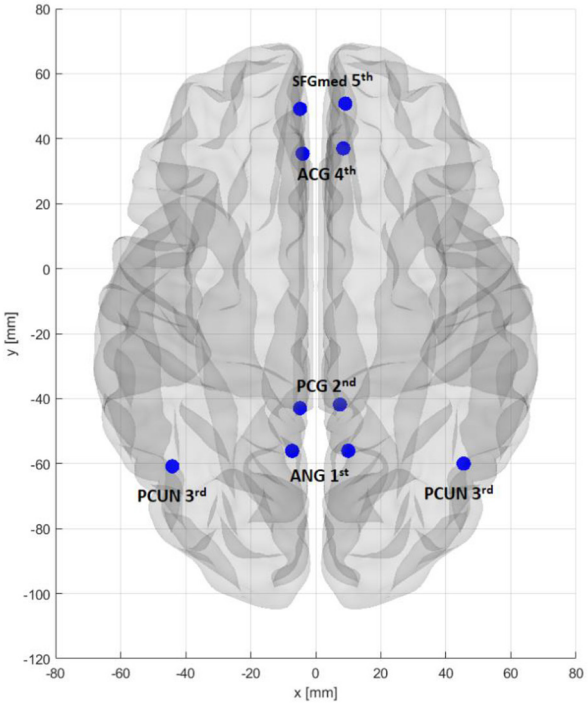

Figure 2: Default Mode Network Regions of Interests (DMN ROIS) and their rank according to significant differences in a statistical test.

Table 5: P-values of the nodal features extracted for the node number 23 in the Automated Anatomical Labeling (AAL) atlas.

Features	P-Values		
Correlation	Pearson	Spearman	Kendall
Triangles	0.0881	0.1149	0.1021
Betweenness	0.4382	0.3613	0.3333
Closeness	0.0730	0.0926	0.0746
Participation	0.0128	0.0121	0.0137

Discussion

This paper aims to investigate and compare the different prevalent correlation methods in generating brain functional graphs. Firstly, the fMRI data of AD patients and control groups were preprocessed and time series were extracted based on AAL atlas. Secondly, the correlation between signals of different ROIs was computed in every subject by 3 different correlation methods. Then, the graph global measures were extracted in the whole brain graph. In another analysis, the global measures were extracted in the DMN network. Moreover, nodal measures in the DMN network were also calculated. In the whole-brain analysis based on global measures, Spearman and Kendall correlations were stronger in discrimination between AD subjects and healthy ones in comparison to the Pearson correlation. Since Spearman and Kendall present more significant difference in global measures in comparison to Pearson, these methods are superior in brain functional connectivity analysis in AD.

It is worthwhile to mention that some features, including eccentricity, radius, and diameter (that calculated based on eccentricity) show no significant changes regardless of the correlation method. On the other hand, some features, showing brain functional integration and segregation such as efficiencies, characteristic path length, clustering, and transitivity show significant changes in all three different correlation methods.

In DMN network analysis employing global measures, again the Spearman and Kendall were more powerful and show more significant difference. Also, the eccentricity feature shows no significant changes in neither the correlation methods nor DMN ROIs. The most disrupted functional connectivity among DMN ROIs was the posterior, including angular, cingulum posterior, and precuneus ROIs, respectively. On the other hand, the frontal ROI's had less functional connectivity disruption. Overall, the left hemisphere shows more significant changes. Since the individuals were right-handed, it can be concluded that the functional connectivity of the dominant hemisphere is disrupted more from AD. In the nodal analysis of DMN ROIs, the triangle and closeness features had the most better performance in distinguishing AD cases from the normal group respectively. Also, the performance of different correlation methods were the same approximately. Besides, the functional connectivity disruption in DMN ROIs based on nodal measures was similar to global measures.

Conclusion

In this study, different correlation methods have been evaluated for brain functional network generation. Although there is no gold standard, the most common method is the Pearson correlation coefficient that has limitations in capturing non-linear dependencies. In the used database, the Spearman and Kendall correlation was more powerful. Accordingly, the weakness of Pearson was demonstrated. For further studies, assessing other methods, especially non linear methods such as distance correlation or mutual information, is highly recommended. Furthermore, the investigation of other databases and different types of binary graphs are suggested as well.

Conflict of Interest

None

References

1. Bijsterbosch J, Smith SM, Beckmann CF. An introduction to resting state fMRI functional connectivity. Oxford University Press; 2017.
2. Rossini PM, Di Iorio R, Bentivoglio M, Bertini G, Ferreri F, Gerloff C, et al. Methods for analysis of brain connectivity: An IFCN-sponsored review. *Clin Neurophysiol.* 2019;**130**(10):1833-58. doi: 10.1016/j.clinph.2019.06.006. PubMed PMID: 31401492.
3. Hull JV, Dokovna LB, Jacokes ZJ, Torgerson CM, Irimia A, Van Horn JD. Resting-state functional connectivity in autism spectrum disorders: a review. *Front Psychiatry.* 2017;**7**:205. doi: 10.3389/fpsyt.2016.00205. PubMed PMID: 28101064.

PubMed PMCID: PMC5209637.

4. Baggio HC, Junqué C. Functional MRI in Parkinson's Disease Cognitive Impairment. *Int Rev Neurobiol*. 2019;**144**:29-58. doi: 10.1016/bs.irn.2018.09.010. PubMed PMID: 30638456.
5. Hua J, Blair NI, Paez A, Choe A, et al. Altered functional connectivity between sub-regions in the thalamus and cortex in schizophrenia patients measured by resting state BOLD fMRI at 7T. *Schizophr Res.* 2019;**206**:370-7. doi: 10.1016/j.schres.2018.10.016. PubMed PMID: 30409697. PubMed PMCID: PMC6500777.
6. Farahani FV, Karwowski W, Lighthall NR. Application of graph theory for identifying connectivity patterns in human brain networks: a systematic review. *Front Neurosci.* 2019;**13**:585. doi: 10.3389/fnins.2019.00585. PubMed PMID: 31249501. PubMed PMCID: PMC6582769.
7. Alzheimer's Association. 2019 Alzheimer's disease facts and figures. *Alzheimer's Dementia.* 2019;**15**(3):321-87. doi: 10.1016/j.jalz.2019.01.010.
8. Forouzannezhad P, Abbaspour A, Fang C, et al. A survey on applications and analysis methods of functional magnetic resonance imaging for Alzheimer's disease. *J Neurosci Methods*. 2019;**317**:121-40. doi:10.1016/j.jneumeth.2018.12.012. PubMed PMID: 30593787.
9. Dennis EL, Thompson PM. Functional brain connectivity using fMRI in aging and Alzheimer's disease. *Neuropsychol Rev.* 2014;**24**(1):49-62. doi: 10.1007/s11065-014-9249-6. PubMed PMID: 24562737. PubMed PMCID: PMC4109887.
10. Gao Y, Li M, Zu Z, Rogers BP, Anderson AW, Ding Z, Gore JC. Progressive degeneration of white matter functional connectivity in Alzheimer's Disease. Proceedings Volume 10953, Medical Imaging 2019: Biomedical Applications in Molecular, Structural, and Functional Imaging; San Diego, California, United States: SPIE; 2019. doi: 10.1117/12.2512919.
11. De Vos F, Koini M, Schouten TM, Seiler S, et al. A comprehensive analysis of resting state fMRI measures to classify individual patients with Alzheimer's disease. *Neuroimage*. 2018;**167**:62-72. doi: 10.1016/j.neuroimage.2017.11.025. PubMed PMID: 29155080.
12. Rathore S, Habes M, Iftikhar MA, Shacklett A, Davatzikos C. A review on neuroimaging-based classification studies and associated feature extraction methods for Alzheimer's disease and its prodromal stages. *Neuroimage.* 2017;**155**:530-48. doi: 10.1016/j.neuroimage.2017.03.057. PubMed PMID: 28414186. PubMed PMCID: PMC5511557.
13. Meszlényi RJ, Buza K, Vidnyánszky Z. Resting state fMRI functional connectivity-based classification using a convolutional neural network architecture. *Front Neuroinform.* 2017;**11**:61. doi: 10.3389/fninf.2017.00061. PubMed PMID: 29089883. PubMed PMCID: PMC5651030.
14. Franzmeier N, Caballero MA, Taylor AN, Simon-Vermot L, Buerger K, et al. Resting-state global functional connectivity as a biomarker of cognitive reserve in mild cognitive impairment. *Brain Imaging Behav*. 2017;**11**(2):368-82. doi: 10.1007/s11682-016-9599-1. PubMed PMID: 27709513.
15. Cai S, Chong T, Peng Y, Shen W, Li J, Von Deneen KM, Huang L. Altered functional brain networks in amnestic mild cognitive impairment: a resting-state fMRI study. *Brain Imaging Behav.* 2017;**11**(3):619-31. doi: 10.1007/s11682-016-9539-0. PubMed PMID: 26972578.
16. Dai Z, Lin Q, Li T, Wang X, Yuan H, et al. Disrupted structural and functional brain networks in Alzheimer's disease. *Neurobiol Aging.* 2019;**75**:71-82. doi: 10.1016/j.neurobiolaging.2018.11.005.m. PubMed PMID: 30553155.
17. Hlinka J, Paluš M, Vejmelka M, Mantini D, Corbetta M. Functional connectivity in resting-state fMRI: is linear correlation sufficient? *Neuroimage*. 2011;**54**(3):2218-25. doi: 10.1016/j.neuroimage.2010.08.042. PubMed PMID: 20800096. PubMed PMCID: PMC4139498.
18. Bowyer SM. Coherence a measure of the brain networks: past and present. *Neuropsychiatric Electrophysiology*. 2016;**2**(1):1-2. doi: 10.1186/s40810-015-0015-7.
19. Chirles TJ, Reiter K, Weiss LR, Alfini AJ, et al. Exercise training and functional connectivity changes in mild cognitive impairment and healthy elders. *J Alzheimers Dis*. 2017;**57**(3):845-56. doi: 10.3233/JAD-161151. PubMed PMID: 28304298. PubMed PMCID: PMC6472271.
20. Zhao J, Ding X, Du Y, Wang X, Men G. Functional connectivity between white matter and gray matter based on fMRI for Alzheimer's disease classification. *Brain Behav.* 2019;**9**(10):e01407. doi: 10.1002/brb3.1407. PubMed PMID: 31512413. PubMed PMCID: PMC6790327.
21. Yamashita KI, Uehara T, Prawiroharjo P, et al. Functional connectivity change between posterior cingulate cortex and ventral attention network relates to the impairment of orientation for time in Alzheimer's disease patients. *Brain Imaging Behav*. 2019;**13**(1):154-61. doi: 10.1007/s11682-018-9860-x. PubMed PMID: 29644521.

22. Mueller SG, Weiner MW, Thal LJ, et al. The Alzheimer's disease neuroimaging initiative. *Neuroimaging Clin N Am*. 2005;**15**(4):869-77. doi: 10.1016/j.nic.2005.09.008. PubMed PMID: 16443497. PubMed PMCID: PMC2376747.
23. Petersen RC, Aisen PS, Beckett LA, et al. Alzheimer's disease neuroimaging initiative (ADNI): clinical characterization. *Neurology*. 2010;**74**(3):201-9. doi: 10.1212/WNL.0b013e3181cb3e25. PubMed PMID: 20042704. PubMed PMCID: PMC2809036.
24. Jack Jr CR, Bernstein MA, Fox NC, et al. The Alzheimer's disease neuroimaging initiative (ADNI): MRI methods. *J Magn Reson Imaging*. 2008;**27**(4):685-91. doi: 10.1002/jmri.21049. PubMed PMID: 18302232. PubMed PMCID: PMC2544629.
25. Yan C, Zang Y. DPARSF: a MATLAB toolbox for" pipeline" data analysis of resting-state fMRI. *Front Syst Neurosci*. 2010;**4**:13. doi: 10.3389/fnsys.2010.00013. PubMed PMID: 20577591. PubMed PMCID: PMC2889691.
26. Tzourio-Mazoyer N, Landeau B, Papathanassiou D, et al. Automated anatomical labeling of activations in SPM using a macroscopic anatomical parcellation of the MNI MRI single-subject brain. *Neuroimage*. 2002;**15**(1):273-89. doi: 10.1006/nimg.2001.0978. PubMed PMID: 11771995.
27. Benesty J, Chen J, Huang Y, Cohen I. Pearson correlation coefficient. Noise Reduction in Speech Processing; Berlin, Heidelberg: Springer Topics in Signal Processing; 2009. p. 1-4. doi: 10.1007/978-3-642-00296-0_5.
28. Myers L, Sirois MJ. Spearman correlation coefficients, differences between. *Encyclopedia of Statistical Sciences*. 2004. doi: 10.1002/0471667196.ess5050.pub2.
29. Akoglu H. User's guide to correlation coefficients. *Turk J Emerg Med*. 2018;**18**(3):91-3. doi: 10.1016/j.tjem.2018.08.001. PubMed PMID: 30191186. PubMed PMCID: PMC6107969.
30. Ehtemami A, Scott R, Bernadin S. A Survey of FMRI Data Analysis Methods. SoutheastCon; USA: IEEE; 2018. p. 1-7.
31. Bullmore E, Sporns O. Complex brain networks: graph theoretical analysis of structural and functional systems. *Nat Rev Neurosci*. 2009;**10**(3):186-98. doi: 10.1038/nrn2575. PubMed PMID: 19190637.
32. Rubinov M, Sporns O. Complex network measures of brain connectivity: uses and interpretations. *Neuroimage*. 2010;**52**(3):1059-69. doi: 10.1016/j.neuroimage.2009.10.003. PubMed PMID: 19819337.
33. Meghanathan N. Assortativity Analysis of Real-World Network Graphs based on Centrality Metrics. *Computer and Information Science*. 2016;**9**(3):7-25. doi:10.5539/cis.v9n3p7.
34. Qian W, Fischer C, Churchill N, Kumar S, et al. Decreased Default Mode Network Functional Connectivity in Alzheimer's Disease Patients with Delusions. *Am J Geriatr Psychiatry*. 2019;**27**(10):1060-8. doi: 10.1016/j.jagp.2019.03.020. PubMed PMID: 31130416.
35. Filippi M, Basaia S, Canu E, Galantucci S, et al. Structural and functional brain connectome architecture in Alzheimer's disease and amnesic mild cognitive impairment patients (P4. 091). *J Neurology*. 2017;**88**(16 Supplement):P4.091.
36. Liang Y, Chen Y, Li H, Zhao T, et al. Disrupted functional connectivity related to differential degeneration of the cingulum bundle in mild cognitive impairment patients. *Curr Alzheimer Res*. 2015;**12**(3):255-65. doi: 10.2174/1567205012666150302155336. PubMed PMID: 25731624.